An Insertable Sensing Technology for Structure Health Monitoring

Ziqian. Yang [(1)], Qingjun. Chen [(2)], Xiuquan. Li [(3)], Cheng. Yuan [(4)], Yi. Ren [(5)], Qingzhao. Kong*

[(1)] *Ph. D candidate, Department of Disaster Mitigation for Structures, Tongji University, Shanghai, 200092, China, 1910262@tongji.edu.cn*

[(2)] *Professor, State Key Laboratory of Disaster Reduction in Civil Engineering, Tongji University, Shanghai, 200092, China, chengj@tongji.edu.cn*

[(3)] *Ph. D candidate, Department of Disaster Mitigation for Structures, Tongji University, Shanghai, 200092, China, lixiuquan_tg@tongji.edu.cn*

[(4)] *Postdoc, Department of Disaster Mitigation for Structures, Tongji University, Shanghai, 200092, China, 20310146@tongji.edu.cn*

[(5)] *Undergraduate student, Department of Disaster Mitigation for Structures, Tongji University, Shanghai, 200092, China, 1750075@tongji.edu.cn*

* ***Corresponding Author,*** *Professor, Department of Disaster Mitigation for Structures, Tongji University, Shanghai, 200092, China, qkong@tongji.edu.cn*

Abstract

Earthquake is one of the natural disasters on the earth. Monitoring and assessing of earthquake-induced structural damage is of great significance to protect human life and properties. This paper proposes an insertable sensing technology to provide quantitative damage evaluation in real time for concrete structures. An insertable sensor named smart socket module (SSM) was designed using a diamond array of four spherical piezoceramic shell (SPS) elements pre-casted in a rectangular module with cement-based grouting material (CGM). SSM functions as a stress wave transmitter and receiver node in concrete. The stress wave propagation characteristics in SSM were studied by using finite element analysis. To further verify the feasibility and capability of using SSM for concrete damage evaluation, two experiments, including active sensing-based crack detection and passive sensing-based impact identification, were carried out. Both numerical and experimental results show that the designed insertable module has great potentials to provide a high sensitivity of sensing earthquake-induced damages and structural dynamic responses for concrete structures.

Keywords: structure health monitoring, smart socket module, spherical piezoceramic shell, sensing approach

1. Introduction

Seismic loads applied on concrete structures could cause local damages on concrete elements, and even lead to whole structural failures. Over the past hundreds of years, earthquake-induced structural damages seriously threaten human life and properties. To ensure the safety of civil infrastructures and provide assessment of structural condition, structural health monitoring (SHM) have been considered as an effective tool to monitor structural real-time information during earthquakes [1-3].

In recent years, structural health monitoring-based technologies have received revolutionized accomplishments which significantly help to ensure the safe operation of civil structures [4-6]. Traditional methods, such as strain sensing, electrical impedance tomography (EIT), and electro-mechanical impedance (EMI), have been widely applied for inspecting and monitoring various structures of their service conditions during past years [7]. However, most of the existing inspection and monitoring methods are insensitive to hairline damages or early-age damages in structures. Ultrasonic guided wave (UGW) is a newly emerging technology for non-destructive testing in the past years [8, 9]. Through the analysis of the signal collected by defect boundary or interface, this method could efficiently identify and localize structural damages, especially for invisible minor cracks. Piezoceramic transducer is the mostly popular transducer used in UGW due to its excellent electromechanical coupling property [10, 11] and wide frequency response. The

transducer can perform both active and passive sensing for the damage profiling and structural vibration analysis. Song et al. designed a piezoceramic-based sensor called embeddable smart aggregate (SA) with a sandwiched structure of a piezoceramic patch and two mated marble blocks. SAs can be distributely pre-embedded in concrete and communicate to each other through stress waves. SA-based technologies have been utilized to monitor the damage conditions of reinforced concrete bridge [12], detect the column damage under blast loads [13], characterize hydration performance of early-age concrete [14], study on stress monitoring the sand-filled steel

tube during impact [15], etc. Recently, a novel embeddable spherical smart aggregate (SSA) was proposed by Kong et al. to enhance the limitation of detecting aperture of SA [16,17]. Because of the spherical geometry design, SSA has the capability of onmi-directional detection, which can generate spherical stress waves in concrete [18]. Though SA and SSA sensors have been successfully employed to laboratory research and field applications in SHM, there is a common drawback that the connection wire of SA/SSA should be carefully fixed when constructing, and could not be alternative while the sensors broken-down, all of these lead to a high cost and additional labor for real projects.

In this paper, the authors present their recent work in designing an insertable sensor called smart socket module (SSM) using for four spherical piezoceramic shell (SPS) in a diamond array for concrete damage diagnosis. SSM can be firmly inserted in premade concrete slots and bring concrete very little to nothing influences to its mechanical properties. Firstly, the fabrication procedures of SSM were illustrated, including assembling SPS array, molding, casting, and cable connecting. Secondly, a numerical simulation was performed to reveal the working principle of SSM when it is used as an actuator for signal generation. Thirdly, two experiments were designed and conducted to demonstrate the SSM functions including structural damage detection and impact identification in concrete beams. In the first one, two inserted SSMs as one actuator and one sensor were utilized to monitor the concrete beam cracks in different heights. A damage index was defined to quantify crack conditions using the signal received by the SSM sensor. In the next experiment, the SSM functionality for sensing structural dynamic response was tested. One inserted SSM was used to identify the impact loads applied on the beam surface. Both numerical and experimental studies give promising results to prove that the designed SSM has great potentials to be safely deployed in concrete structures and provide real-time information for earthquake-induced damages and structural dynamic responses.

2. Piezoelectric effect of spherical piezo sensor

Piezoelectric effect was introduced by the brothers Pierre Curie and Jacques Curie, in 1880 [19]. piezoelectricity includes both the direct effect and the inverse effect. The direct effect means the generation of electrical charge when the material subjected to stress. Conversely, the inverse effect refers to the generation of strain while the object was applied by an electric field. Lead zirconate titanate (PZT), as one of the piezo materials, has been made to transducers with various shapes in SHM, such as patch, cylinder, spherical shell, etc. Compared to other PZT shapes, spherical PZT shell is able to facilitate the availability and capability in three dimensions. The detailed properties of PZT are shown in Table 1. The constitutive equation of the spherical piezo shell in spherical coordinate system is given below [16]:

$$\sigma_{rr} = c_{33}\varepsilon_{rr} + 2c_{13}\varepsilon_{\theta\theta} - e_{33}E_r \tag{1}$$

$$\sigma_{\varphi\varphi} = c_{13}\varepsilon_{rr} + \left[c_{11} + c_{12}\right]\varepsilon_{\theta\theta} - e_{31}E_r \tag{2}$$

$$\sigma_{\varphi\varphi} = \sigma_{\theta\theta} \tag{3}$$

$$D_r = e_{33}\varepsilon_{rr} + 2e_{31}\varepsilon_{\theta\theta} + \varepsilon_{rr}E_r \tag{4}$$

where σ_{rr} , $\sigma_{\varphi\varphi}$, $\sigma_{\theta\theta}$ are the stress components along the radial, polar angle and azimuthal angle, respectively. ε_{rr} , $\varepsilon_{\theta\theta}$ are the strain components along the radial and azimuthal angle, respectively. E_r is the

radial electric field, D_r is the radial electric displacement. c_{ij} is the elastic constant, e_{ij} is the piezoelectric coefficient. The stiffness matrix and the piezoelectric stress matrix are symmetrical, namely $c_{ij} = c_{ji}$, $e_{ij} = e_{ji}(i, j=1,2,3)$.

Table 1 – Material properties of the spherical piezoceramic shell

Material type	Density (10^3kg/m^3)	Young's modulus (GPa)	Poisson's ratio	Piezoelectric strain coefficients		Relative dielectric constant
				d_{33} (10^{-10}m/V)	d_{31} (10^{-10}m/V)	ε^T_{r3}
PSnN-5	7.7	65	0.36	4.5	-1.6	1600

3. Fabrication and working principle of the Smart Socket Module (SSM)

3.1 Fabrication procedure

To generate omni-directional stress waves in the detecting field, a spherical piezoceramic shell (SPS) is utilized in SSM design. Four SPSs were firstly coated with epoxy resin as a layer of waterproof and electric isolation. A copper tube was used to protect SPS wire and fix the SPS when casting and eliminate signal noise while working. Four SPSs were arranged in a diamond array and installed in a casting mold made of acrylic in advance, as shown in Fig.1(a).

Secondly, a SSM was fabricated by casting cement-based grouting material (CGM) to the mold. During the casting process, slight vibration is necessary to guarantee intimate contact at the interface between SPS and CGM. Since the CGM performs high-strength and self-compaction properties, and provides extraordinary continuous interface to normal concrete. After curing process, the mold was removed from the module, and a plug-in panel with a Bayonet Neill-Concelman (BNC) connector was placed on the module. Fig.1(b) shows a photo of an assembled SSM.

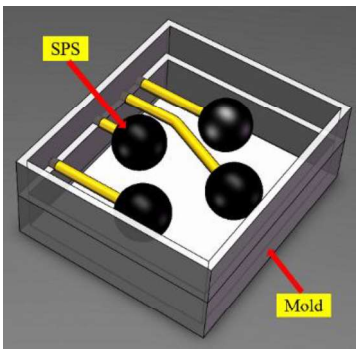

(a) SPSs arraying in mold

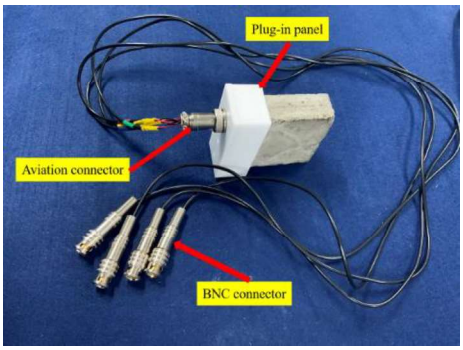

(b) An assembled SSM

Fig. 1 – Fabrication procedure of an SSM

3.2 Working principle

A numerical simulation in Abaqus was performed to analyze the working principle of SSM as a stress wave actuator. In the finite element model, a Gaussian pulse was simultaneously applied to each SPS. The wavefield distributions at two moments are shown in Fig.2. At time equals to 4.12ms, it can be seen that four

SPSs simultaneously transmitted stress waves outward. When reaching 5.04ms, four waves were superimposed on the surface of the SSM, and an energy focusing region appears in the center of the surface. According to the superposition principle, when the SSM was inserted in concrete, it can transmit the probe signal in the form of the superimposed waves to concrete.

(a) Time = 4.12ms (b) Time = 5.04ms

Fig. 2 – The wave field distributions during stress wave generation process

4.Experiment

4.1 Experiment 1: Active-sensing for damage profiling

4.1.1 Experimental setup

An experiment was carried out to verify the capability of SSM for damage profiling. A total of four concrete beam specimens, including one intact concrete beam and three damaged beams with 3cm, 6cm, and 9cm height of crack in the middle section were prepared. The length, width, and height of the beam are 700mm, 120mm, and 180mm, respectively. For each beam, two rectangular slots were reserved to install SSMs. Fig.3(a) shows the installation schematic of SSM1 and SSM2 for each beam. The detailed information of SPSs with label No. are given in Fig.3(b). In this experiment, the SSM2 was utilized as a generator to excite a probe signal. Meanwhile, the SSM1 was chosen as the sensor to receive the signal propagated from SSM2. The experimental setup is presented in Fig.4. The intact concrete beam and the other ones with cracks of 3cm, 6cm, and 9cm beams are defined as case1 to case4, as shown in Fig. 5. The excited signal used in this experiment is a sine sweeping wave with the period, amplitude, frequency range of 0.5s, 150V, 1kHz to 50kHz, respectively.

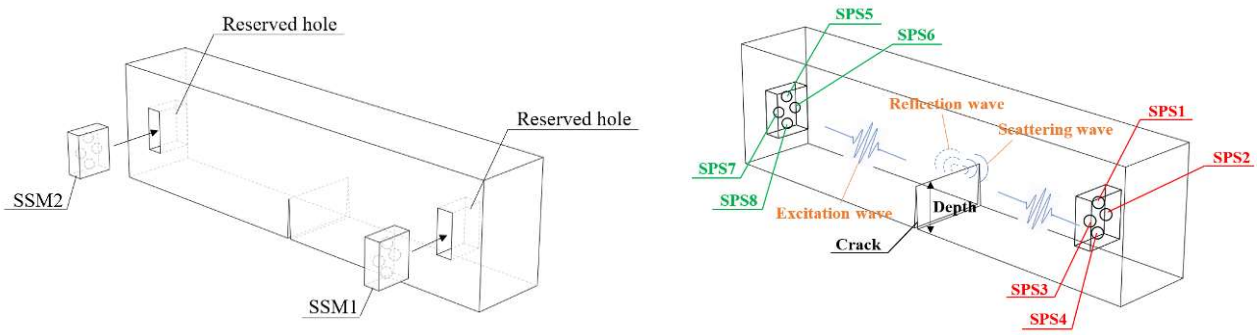

(a) Inserting the SSMs into concrete beam (b) Perspective of SSM sensing in beam

Fig. 3 – Schematic of SSM working

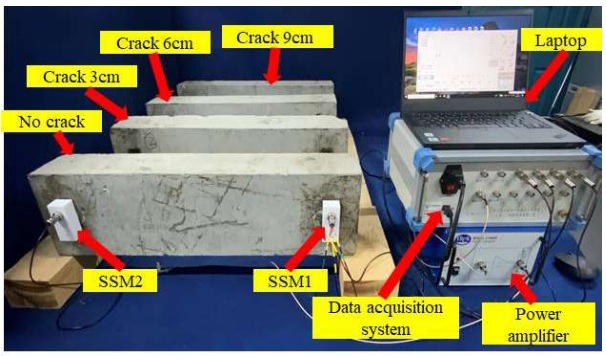

Fig. 4 – Experimental setup

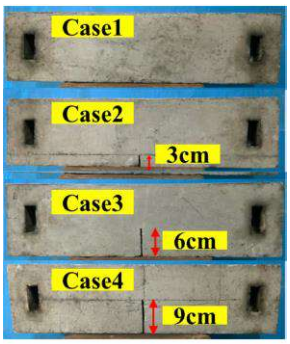

Fig. 5 – Four cases of the beam specimens

4.1.2 Damage index for crack condition evaluation

A damage index was defined to evaluate the damage quantitively. The received signal was firstly decomposed into 2^n sets by a signal processing tool of wavelet packet decomposition:

$$\left\{X_1, X_2, \ldots X_{2^n}\right\} \tag{5}$$

In each set, $X_i\left(i=1,2,\ldots 2^n\right)$ can be decomposed as:

$$X_i = \left[X_{i,1}, X_{i,2}, \ldots, X_{i,m}\right] \tag{6}$$

where m is the number of data samples. The energy of each set can be defined as:

$$E_i = \sum_{j=1}^{m} X_{i,j}^2 \tag{7}$$

The total energy can be acquired by summing of E_i:

$$E_{tot} = \sum_{i=1}^{2^n} E_i \tag{8}$$

The damage index I can be defined as:

$$I_k^s = 1 - E_{tot,k}^s / E_{tot,1}^s \tag{9}$$

where $E_{tot,k}^s$ means the total energy received by s^{th} SPS in k^{th} case (s,k = 1,2,3,4). When $E_{tot,k}^s = E_{tot,1}^s$, the signal is identical to the original signal. It can be obtained I=0, which means the structure is very close to intact condition. While $E_{tot,k}^s = 0$, i.e., I=1, the structure appears the penetrating crack or states in a severe damage condition. The stress waves cannot be received by the sensor.

4.1.3 Experimental results

All SPSs in SSM2 generated the same probe signal simultaneously. SPS1 to SPS4 in SSM1 received the signal response individually. The same test procedures were carried out on each beam specimen. Fig.6 shows

the response signals received by each SPS in SSM1 for the four cases. The damage index of each SPS for all cases and the average values of all SPSs in each case were computed and drawn in Fig. 7.

From fig.7, it can be seen that, both damage index values from each single SPS and the average value, the increases monotonically with the growth of crack height. In case 2, the value is very close to 0, which agrees with the specimen condition that the crack occurs at the bottom of the beam (crack = 3cm). After that, the damage index value ascends sharply from case 2 to case 3. Correspondingly, the crack depth increases from 3cm to 6cm which is one third of the total beam height. In case 4, the damage index value rises to about 0.8, which implies that the beam is in a severe damage condition. Correspondingly in this case, the crack depth of the beam is 9cm, which is half of the total beam height.

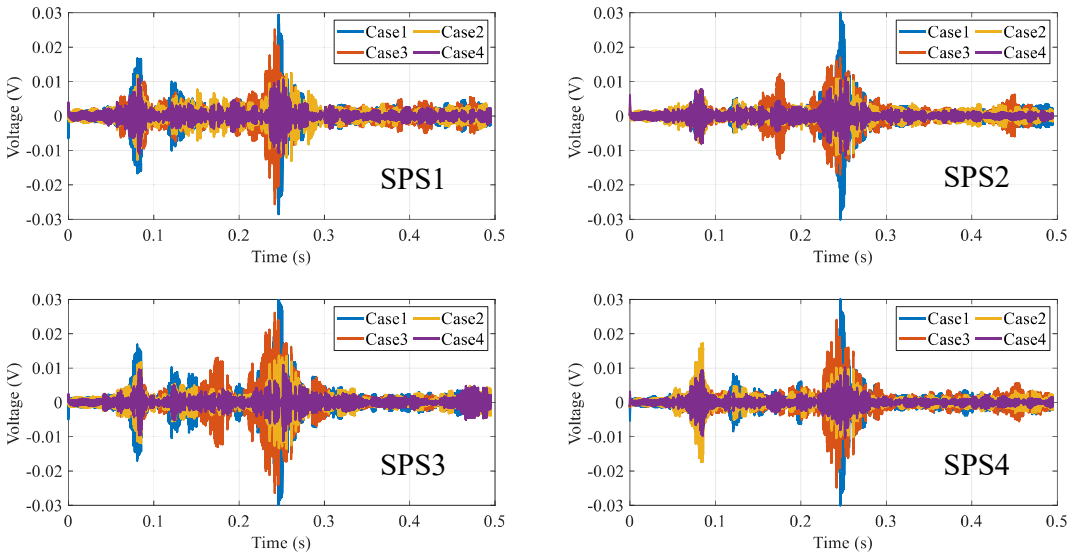

Fig. 6 – Time-domain signal of each SPS in SSM1 under different cases

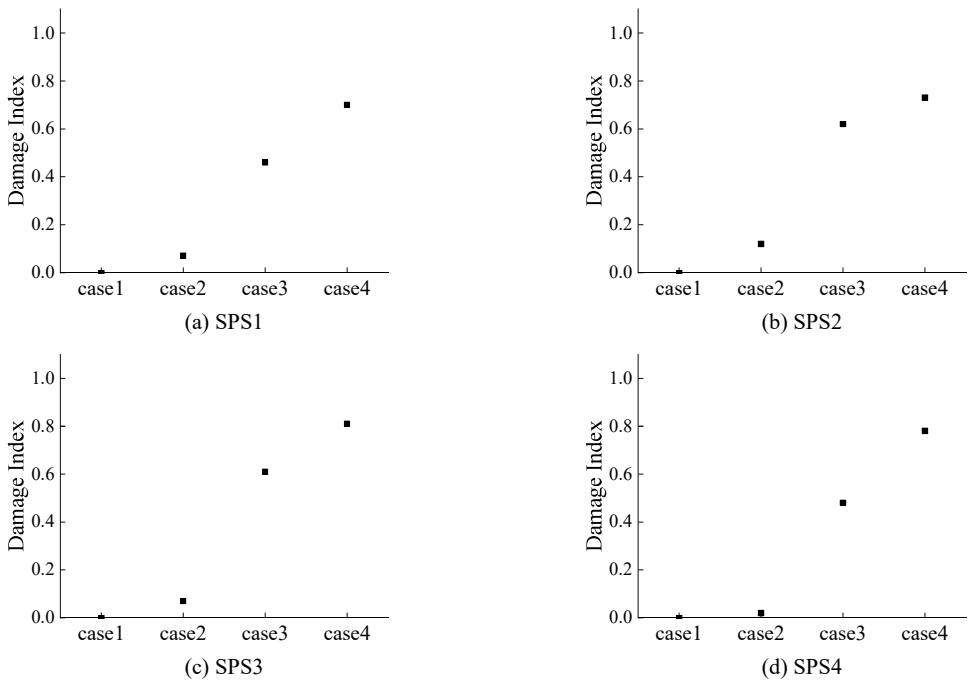

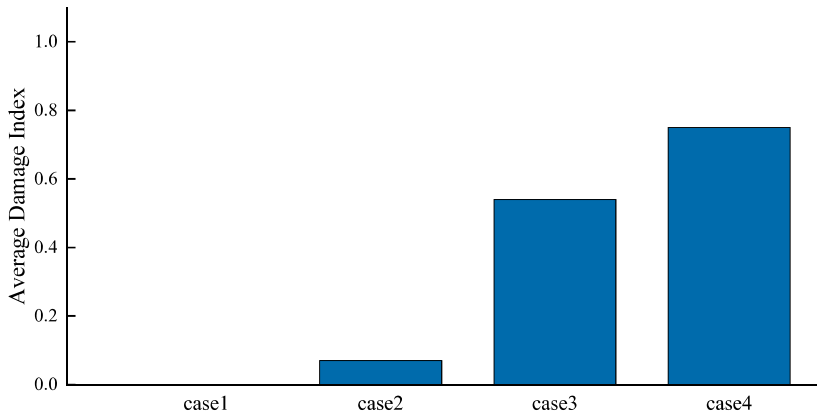

(e) Average of Four SPSs

Fig. 7 – Damage index

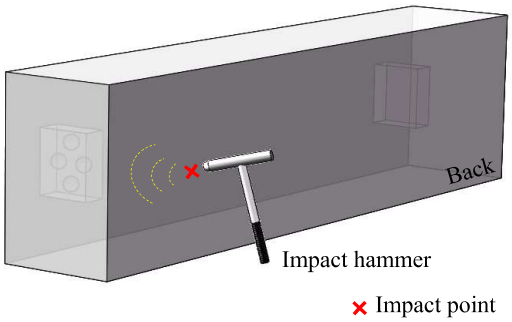

(a) Wave propagation schematic

(b) Impact generation with an impact hammer

Fig. 8 –Experiemental setup for impact identification

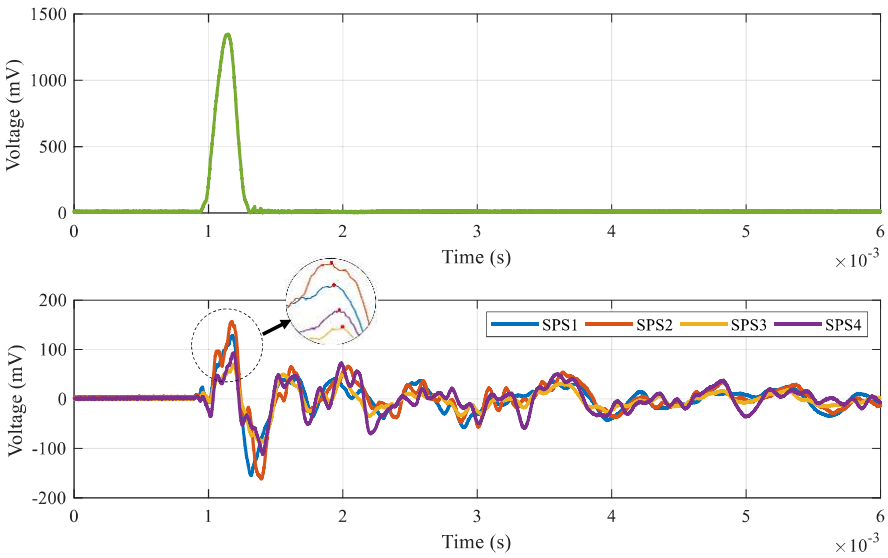

Fig. 9 – Excitation impact hammer signal and received signal from all SPSs

4.2 Experiment 2: Impact identification

To investigate the passive sensing capability of SSM, an impact experiment was also implemented in this research. The experimental schematic is shown in Fig.8. In this study, SSM1 was used as a sensor. An artificial impact was generated by an impact hammer on the projection point of SSM1 in the back side of the beam. Fig.9 shows the excited impact signal and received signal from each SPS. It can be clearly seen the impact event can be clearly captured by all SPSs in the tested SSM. Furthermore, it is visually obtained that SPS2 received the maximum peak value because of the minimum stress wave attenuation path between impact point and SPS2. The interval of arriving time would be studied for impact localization in the future research.

5.Conclusion

In this paper, an innovative insertable sensing module called SSM was designed and tested. A detailed fabrication procedure was introduced. The numerical simulation revealed that the SSM could generate superimposed waves to enhance the probe signal strength which could help to improve the crack detection accuracy. In the first experiment, results show that the damage index values increase monotonically with the growth of crack height in the concrete beam specimens. The feasibility of using SSMs for damage profiling was verified. In the second experiment, each SPS in the tested SSM can clearly captured the impact event, which verified the capability of using SSM for sensing structural dynamic response. In the authors' future work, crack imaging technology will be studied for crack reconstruction by using SPS array. In addition, the impact localization technology will also be studied to determine the impact location of the structure with inserted SSM.

6. References

[1] X.C. Lin, M. Kato, L.X. Zhang, M. Nakashima (2018): Quantitative investigation on collapse margin of steel high-rise buildings subjected to extremely severe earthquakes. *Earthq. Eng. Eng. Vib.,* 17, 445-457.
[2] M. Nakashima, H. Kato, E. Takaoka (1992): Development of real-time pseudo dynamic testing. 21, 79-92.
[3] M. Nakashima, K. Ogawa, K.J.E.E. Inoue, S. Dynamics (2010): Generic frame model for simulation of earthquake responses of steel moment frames. 31.
[4] J. Chen, P. Li, G.B. Song, Z. Ren, Y. Tan, Y. J.Zheng (2018): Feedback Control for Structural Health Monitoring in a Smart Aggregate Based Sensor Network. International Journal of Structural Stability and Dynamics, 18, 5.
[5] C.R. Farrar, K. Worden (2007): An introduction to structural health monitoring. *Philos. Trans. R. Soc. A-Math. Phys. Eng. Sci.,* 365, 303-315.
[6] I.P. Kang, M.J. Schulz, J.H. Kim, V. Shanov, D.L. Shi (2006): A carbon nanotube strain sensor for structural health monitoring. *Smart Materials and Structures,* 15, 737-748.
[7] C. Kralovec, M. Schagerl (2020): Review of Structural Health Monitoring Methods Regarding a Multi-Sensor Approach for Damage Assessment of Metal and Composite Structures. 20, 826.
[8] J.L. Rose, Ultrasonic Guided Waves in Solid Media, Cambridge Univ Press, Cambridge, 2014.
[9] Z.Q. Su, L. Ye, Y. Lu (2006): Guided Lamb waves for identification of damage in composite structures: A review. *J. Sound Vibr.,* 295, 753-780.
[10] J.W. Ayres, F. Lalande, Z. Chaudhry, C.A. Rogers (1998): Qualitative impedance-based health monitoring of civil infrastructures. *Smart Materials & Structures,* 7, 599-605.
[11] B.T. Wang, R.L. Chen (2000): The use of piezoceramic transducers for smart structural testing. *J. Intell. Mater. Syst. Struct.,* 11, 713-724.
[12] C.K. Soh, K.K.H. Tseng, S. Bhalla, A. Gupta (2000): Performance of smart piezoceramic patches in health monitoring of a RC bridge. *Smart Materials & Structures,* 9, 533-542.
[13] K.Xu, Q. S.Deng, L. J.Cai, S. C. Ho, G. B. Song (2018): Damage Detection of a Concrete Column Subject to Blast Loads Using Embedded Piezoceramic Transducers. Sensors, 18, 5.

[14] Q.Z. Kong, S. Hou, Q. Ji, Y.L. Mo, G.B. Song (2013): Very early age concrete hydration characterization monitoring using piezoceramic based smart aggregates. *Smart Materials and Structures,* 22, 7.
[15] G.F. Du, J. Zhang, J.C. Zhang, G.B. Song (2016): Experimental Study on Stress Monitoring of Sand-Filled Steel Tube during Impact Using Piezoceramic Smart Aggregates. Sensors, 17, 8.
[16] Q.Z. Kong, S.L. Fan, X.L. Bai, Y.L. Mo, G.B. Song (2017): A novel embeddable spherical smart aggregate for structural health monitoring: part I. Fabrication and electrical characterization. *Smart Materials and Structures,* 26, 8.
[17] Q.Z. Kong, S.L. Fan, Y.L. Mo, G.B. Song (2017): A novel embeddable spherical smart aggregate for structural health monitoring: part II. Numerical and experimental verifications. *Smart Materials and Structures,* 26, 9.
[18] J.J. Wang, Q.Z. Kong, Z.F. Shi, G.B. Song (2018): A Theoretical Model for Designing the Novel Embeddable Spherical Smart Aggregate. *IEEE Access,* 6, 48403-48417.
[19] https://en.wikipedia.org/wiki/Piezoelectricity.

